

# DC-Bus Voltage Control for Three-Phase Bi-directional Inverter in DC Microgrid Applications

T.-F. Wu, C.-H. Chang, L.-C. Lin, and Y.-C. Chang  
Elegant Power Application Research Center (EPARC)  
Department of Electrical Engineering  
Nation Chung Cheng University  
Ming-Hsiung, Chia-Yi, Taiwan, R.O.C.  
E-mail: [ieetfwu@ccu.edu.tw](mailto:ieetfwu@ccu.edu.tw)

**Abstract**—This paper presents dc-bus voltage control for a three-phase bi-directional inverter in dc-microgrid applications. The bi-directional inverter can fulfill both grid connection and rectification modes with power factor correction. The proposed control includes two approaches, one line-cycle regulation approach (OLCRA) and one-sixth line-cycle regulation approach (OSLCRA), which take into account dc-bus capacitance and regulate dc-bus voltage to track a linear relationship between dc-bus voltage and inverter inductor current. With the OLCRA, the inverter can tune the dc-bus voltage to the desired voltage accurately every line cycle, which can reduce the frequency of operation mode change and current distortion. The OSLCRA adjusts current command every one-sixth line cycle to adapt to abrupt dc-bus voltage variation. The two approaches together can prevent dc-bus voltage from dramatic change and improve the availability of the dc-microgrid without increasing dc-bus capacitance. Determination of dc-bus capacitance is also presented in this paper. Experimental results measured from a 10 kVA three-phase bi-directional inverter have verified the feasibility of the discussed control approaches.

## I. INTRODUCTION

Grid-connected systems based on a two-stage configuration have been widely studied. Recently, dc distributed generation systems, as shown in Fig.1, have been being emerging [1]. They can draw maximum power from renewable sources and inject the power into utility grid with unity power factor, or they can rectify the ac source to replenish and regulate the dc bus. Therefore, the control of dc-bus voltage is an important issue to dc-microgrid designers.

In the past studies, the voltage control based on gain-scheduling was presented [2]-[4], which uses a droop concept to design proper dc gain. Moreover, some attempts combining

the gain-scheduling with fuzzy control were also discussed [5]-[6], which incorporate fuzzy control and adjust dc voltage reference to balance power flow. Then, other dc-bus voltage controls, such as robust, adaptive, and hybrid control [7]-[9] to enhance system stability were reported. However, a dc microgrid requires a power management scheme to improve system availability [10]; that is, it is allowed to have a certain range of dc-bus voltage variation for both grid-connection and rectification modes. When the system is operated in grid-connection mode, it needs a higher dc-bus voltage to prevent dramatic voltage drop below the lower bound due to a step dc load increase. On the contrary, it requires a lower dc-bus voltage to extend the range of voltage swing in rectification mode. In the literature, the approaches for achieving fast dc-bus voltage dynamics were focused on the systems without dc-load [11]-[12], while there is no control for the bi-directional inverter systems with abrupt dc load variation.

In our previous research [13], a digital predictive controlled 10 kVA 3  $\phi$  bi-directional inverter with wide inductance variation has been designed and implemented. Based on its configuration, this paper presents two dc-bus voltage regulation approaches, one line-cycle regulation approach (OLCRA) and one-sixth line-cycle regulation approach (OSLCRA), which are based on a linear power management scheme. The OLCRA updates the current commands every line cycle at the zero-crossing of a specified phase, and it can reduce the frequency of operation mode change and current distortion significantly. The OSLCRA will update the current command every one-sixth line cycle to avoid over/under dc-bus voltage fault due to abrupt dc load variation, which can improve the availability of the dc microgrid without increasing dc-bus capacitance. With the two control approaches, the bi-directional inverter can tune current commands and the two operation modes to balance power

flow, and to achieve a linear relationship between inverter current and dc-bus voltage. Furthermore, this paper also discusses the design of dc-bus capacitance, since the two approaches take into account the dc-bus capacitance to derive the control laws. The dc-bus capacitance can be minimized for reducing system size and cost. Experimental results measured from a 10 kVA 3 $\phi$  bi-directional inverter are presented to confirm the proposed approaches.

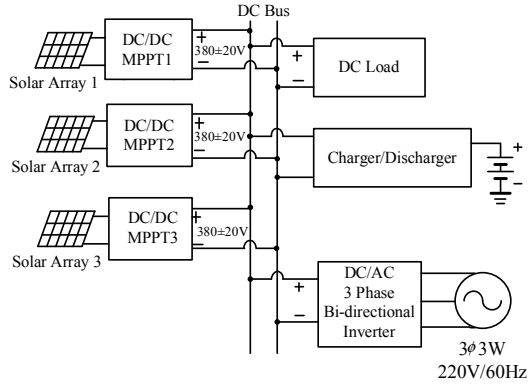


Figure 1. Configuration of a dc microgrid application system.

## II. DC-BUS VOLTAGE CONTROL

A system diagram of the discussed three-phase bi-directional inverter is shown in Fig. 2. It can fit to both delta-connected and Y-connected ac grid. In the designed prototype, *Renesas* micro-chip *RX62T* is adopted for realizing the system controller, which has 1.65 MIPS and includes floating calculation and division. By considering wide inductance variation [13], the inverter can be operated stably, especially in high current applications. However, the system requires dc-bus voltage control scheme for balancing power flow. The concepts include linear power management scheme, one line-cycle regulation approach, and one-sixth line-cycle regulation approach.

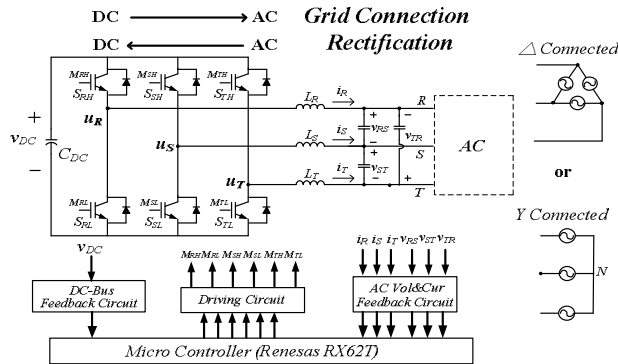


Figure 2. System diagram of the proposed three-phase bi-directional inverter.

### A. Linear Power Management Scheme

Fig. 3 shows an illustration of the proposed linear power management scheme for achieving a linear relationship between inductor current  $i_L$  and dc-bus voltage  $v_{DC}$ . The operating range of the dc-bus voltage is  $380 \pm 20$  V. When

the inverter is operated in grid-connection mode (selling power), the operating range is from 380 V to 400V, which insures an enough voltage level to accommodate abrupt dc load increase. On the other hand, when the inverter is operated in rectification mode (buying power), the low voltage range, 380 V ~ 360 V, can enhance mode stability when fast dc load drop.

Fig. 3 also shows the locus of the dc-bus voltage regulation sequence in grid-connection mode. At time  $t_0$ , the inverter stays at operation point  $(v_{DC}(n-1), I_A(n-1))$  on the load line, where  $I_A$  is the adjustable current command which is tuned every line cycle with the OLCRA. The operation point will move away from the load line to point  $(v_{DC}(n), I_A(n-1))$  at  $t_1$  when there exists power imbalance. Then, the controller will update current command  $I_A(n-1)$  with  $I_A(n)$  at the start of the  $n^{th}$  line cycle, which will regulate dc-bus voltage to a new set-point voltage  $v_{DC}(n+1)$  according to the linear power management scheme. When the inverter reaches operation point  $(v_{DC}(n+1), I_A(n))$  at  $t_2$ , the controller will change current command to  $I_A(n+1)$ , maintaining dc-bus voltage  $v_{DC}$  for a new power balance. The system will be operated in the new steady state after time  $t_3$ . Its control law will be derived in the following section.

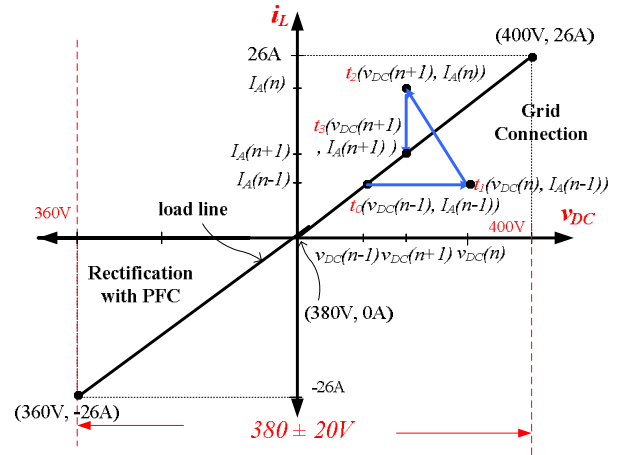


Figure 3. Illustration of a linear power management scheme for achieving a linear relationship between inductor current  $i_L$  and dc-bus voltage  $v_{DC}$ .

### B. One Line-Cycle Regulation Approach

Fig. 4 shows a diagram for illustrating the OLCRA when power imbalance is occurring. In Fig. 4, power imbalance happens at time  $t_{x1}$ , and dc-bus voltage will increase from  $v_{DC}(n-1)$  to  $v_{DC}(n)$ . At time  $t_n$ , dc-bus capacitor current variation  $\Delta i_C$  can be determined as:

$$\Delta i_C = C_{DC} \frac{v_{DC}(n) - v_{DC}(n-1)}{t_n - t_{x1}} \quad (1)$$

However, time  $t_{x1}$  is unpredictable, and an initial guess is made to  $t_{n-1}$ ; thus, new current command  $I_A(n)$  for time interval  $[t_n, t_{n+1}]$  can be determined based on previous current  $I_A(n-1)$  as:

$$I_A(n) = I_A(n-1) + \frac{C_{DC}(v_{DC}(n+1) - v_{DC}(n-1))}{T_l}, \quad (2)$$

where  $T_l$  is a line period and  $v_{DC}(n+1)$  is the set-point voltage which can be derived based on the relationship shown in Fig. 3 as follows:

$$v_{DC}(n+1) = 380 + \frac{20V}{26A} I_A(n), \quad (3)$$

where

$$I_A(n) = I_A(n-1) + \frac{C_{DC}(v_{DC}(n) - v_{DC}(n-1))}{T_l}. \quad (4)$$

In the above equations,  $I_A(n)$  is always used for regulating dc-bus voltage to set-point voltage  $v_{DC}(n+1)$  according to the control diagrams shown in Fig. 3 and Fig. 4. Current command  $I_A(n)$  will be tuned every line cycle for maintaining dc-bus voltage  $v_{DC}(n)$  to the desired voltage on the load line. The inverter controller will update current command  $I_A(n)$  cycle by cycle; that is,  $I_A(i)$  will be equal to  $I_A(i-1)$  after the new current command has been determined at the beginning of a line cycle. In Fig. 4, if a power imbalance occurs at  $t_{x1}$  (curve 1) or another one occurs at  $t_{x2}$  (curve 2), the inverter will tune current command  $I_A$  continuously until  $v_{DC}$  comes back to the load line shown in Fig. 3, achieving power balance on dc bus. The overall control block diagram is shown in Fig. 5.

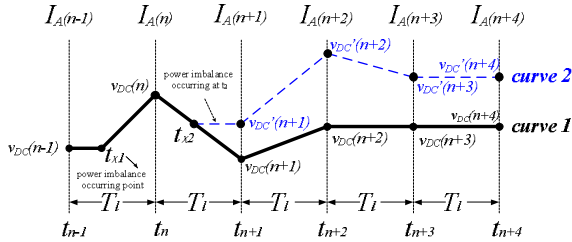


Figure 4. Illustration of the OLCRA to dc-bus voltage regulation for the inverter with power imbalance.

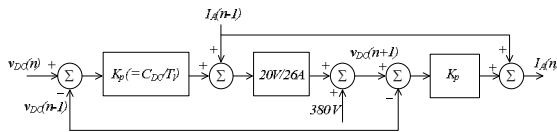


Figure 5. Control block diagram of the proposed OLCRA.

### C. One-Sixth Line-Cycle Regulation Approach

When dc loads change suddenly, the OLCRA cannot regulate dc-bus voltage immediately, and it needs a fast dynamic current control to balance the power flow. In a three-phase inverter system, the fast regulation interval is selected to be one-sixth line-cycle, because the frequency of dc-bus voltage ripple  $v_r$  is six times line frequency as shown in Fig. 6. From Fig. 6, it can be observed that the start-points of dc-bus voltage in all six regions are identical, and we can realize the control scheme without the consideration of dc-bus voltage ripple. Moreover, the ripple of inverter input equivalent

current  $i_{inv}$ , about  $0.134i_L (=1.0i_L - 0.866i_L)$ , is much smaller than that in a single-phase inverter system, and it can be even ignored for the control law derivation, as denoted with curve 1 and shown in Fig. 7.

Fig. 7 illustrates the current tuning process of the proposed OSLCRA. With the OSLCRA, the inverter will update current command  $I_A$  at the beginning of each one-sixth line-cycle to drive dc-bus voltage to set-point voltage  $v_{DC}(n+1)$  at time  $t_{n+1}$ . Thus, according to a dc-bus voltage variation, the current-command control law can be derived as follows:

$$I_A\left(n + \frac{i}{6}\right) = \frac{6C_{DC}\Delta v_i}{T_l} + I_A(n), \quad (5)$$

where  $i = 1, 2, \dots, 5$ ,

$$\Delta v_i = v_{DC}\left(n + \frac{i}{6}\right) - v_{DC}\left(n + \frac{(i-1)}{6}\right) - \frac{v_{DC}(n+1) - v_{DC}\left(n + \frac{i}{6}\right)}{6-i}. \quad (6)$$

Voltage variation  $\Delta v_i$  includes two portions: one is the variation between one-sixth cycles  $\left(v_{DC}\left(n + \frac{i}{6}\right) - v_{DC}\left(n + \frac{(i-1)}{6}\right)\right)$  and the other is the average difference between  $v_{DC}(n+1)$  and the current point  $\left(\frac{v_{DC}(n+1) - v_{DC}\left(n + \frac{i}{6}\right)}{6-i}\right)$ . The first variation is caused by

abrupt power imbalance, of which the dc-bus voltage will deviate from the load line. By adding this variation to current command in one-sixth cycle, the inverter can balance power flow substantially, but dc-bus voltage  $v_{DC}$  still does not reach its set point yet. Thus, the second term is used for regulating  $v_{DC}$  to voltage  $v_{DC}(n+1)$  which has been determined at the beginning of the  $n^{\text{th}}$  line cycle, as shown in (3). With the compensation of the two portions, the dc-bus voltage will come back to the load line after power imbalance occurs at  $t_{y1}$  (curve 2) or  $t_{y2}$  (curve 3), as shown in Fig. 7. It can be observed that the inverter controller updates current

command  $I_A\left(n + \frac{1}{6}\right)$  at  $t_n + \frac{1}{6}T_l$  after dc-bus voltage drops abruptly at  $t_{y1}$  (curve 2). However, the inverter controller will determine a wrong current command due to the unpredicted time  $t_{y1}$ , and the dc-bus voltage will not be regulated to a correct voltage value until next one-sixth line cycle,  $t_n + \frac{2}{6}T_l$ .

If a new power imbalance occurs at  $t_{y2}$  (curve 3), the same regulating process will happen again. That is, the inverter will use a correct current command  $I_A\left(n + \frac{3}{6}\right)$  to regulate the dc-bus voltage to a set-point voltage.

Furthermore, current command  $I_A(n)$  must be modified for determining command  $I_A(n+1)$  at the beginning of a new cycle due to the one-sixth line-cycle command change, and it is just equal to the average value of all current commands

within the time interval of  $[t_n, t_{n+1}]$ . The determination of current command  $I_A(n)$  can be rewritten as:

$$I_A(n) = \frac{I_A(n-1) + \sum_{i=1}^5 I_A\left(n + \frac{i}{6}\right)}{6} \quad (7)$$

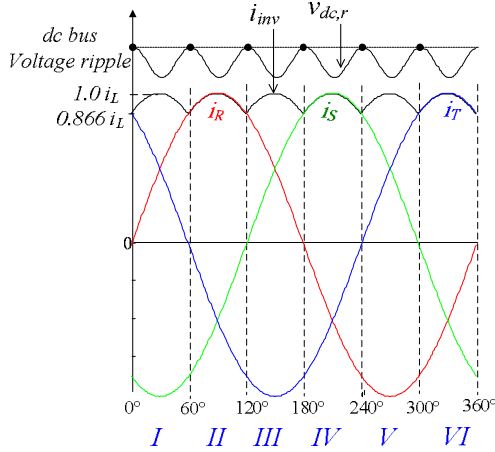


Figure 6. Illustration of three-phase line current  $i_R$ ,  $i_S$  and  $i_T$ , inverter input current  $i_{inv}$ , and dc-bus voltage ripple  $v_r$ .

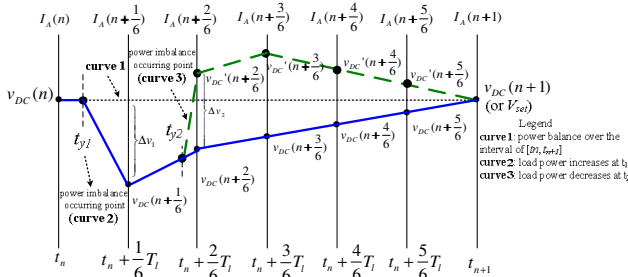


Figure 7. Illustration of the OSLCRA to dc-bus voltage regulation for the inverter under power imbalance.

### III. DESIGN OF DC-BUS CAPACITANCE

Since the current-command control laws include the parameter of dc-bus capacitance, the two approaches can regulate the dc bus to the desired voltage. It needs to determine the dc-bus capacitance first. The dc-bus capacitance is related to the current injected into the capacitor and the dc-bus voltage variation, and it can be expressed as

$$C_{DC} = \frac{\Delta i_c \cdot \Delta t}{\Delta v_{DC}} \quad (8)$$

where  $\Delta i_c$  is the capacitor current variation over time interval  $\Delta t$ ,  $\Delta v_{DC}$  is the dc-bus voltage variation, and  $C_{DC}$  is the dc-bus capacitance. Fig. 8 shows a plot of dc-bus capacitor  $C_{DC}$  versus dc-bus voltage variation  $\Delta v_{DC}$  under a maximum power change of 10 kW and within one-sixth line cycle; that is, capacitor current variation  $\Delta i_c$  is equal to 26.3 A (10 kW/380 V) over the time interval  $\Delta t$  of  $T/6$ . For system availability, dc-bus voltage varying over the upper-bound voltage is not allowed. Thus, the voltage variation must be lower than 20 V

(400 V – 380 V or 380 V – 360 V) within one-sixth line cycle, and  $12 \cdot 470 \mu\text{F}$  capacitance can be selected to fit the appropriate range of dc-bus voltage variation, 10 ~ 15 V. This set of capacitors was used in the experiment.

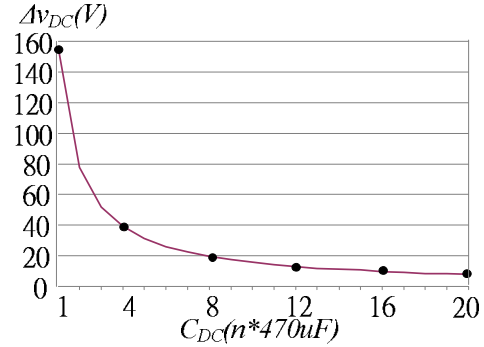


Figure 8. Plot of dc-bus capacitor  $C_{DC}$  versus dc-bus voltage variation  $\Delta v_{DC}$  under a 10 kW abrupt change and within one-sixth line cycle.

### IV. EXPERIMENTAL RESULTS

The proposed dc-bus voltage control has been confirmed by a 10 kVA three-phase bi-directional inverter in a dc distribution system. Based on the aforementioned specifications and analyses, design of the power stage is summarized in Table I. The range of dc-bus voltage is specified from 360 V to 400 V. The nominal  $3 \phi$  line to line voltage is 220 V<sub>rms</sub> and the line frequency is 60 Hz. The inverter inductance varies from 2 mH to 300  $\mu\text{H}$  per phase and the switching frequency is 20 kHz. The power diodes are realized with silicon carbide, which have no reverse-recovery time. A photograph of the designed bi-directional inverter is shown in Fig. 9.

From the previous research [13], Figs. 10 and 11 show the inductor current waveforms of the inverter under the digital predictive control with and without considering wide inductance variation. The tests were based on the inverter operated in grid-connection mode. At 5 kW power level, as shown in Fig. 10, it can be seen that there is a little distortion at the peak current without considering inductance variation, while their difference is not significant at all. However, when the inverter is operated with 10 kW, the measured inductor currents, as shown in Fig. 11, from the control without considering wide inductance variation have large distortion near the peak and a divergence in phase R.

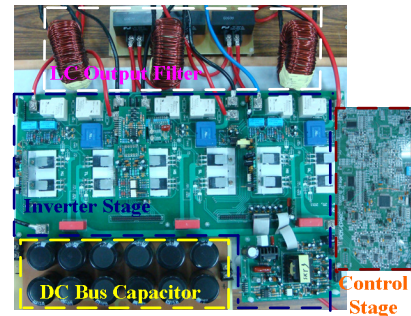


Figure 9. Photograph of the prototype of the designed three-phase bi-directional inverter system.

TABLE I. SYSTEM PARAMETERS OF THE DESIGNED INVERTER PROTOTYPE

Parameters	Symbols	Values
DC-bus voltage	$v_{DC}$	360 ~ 400 V
AC grid voltage	$v_{RS}, v_{ST} \& v_{TR}$	220 V <sub>rms</sub> (nominal)
Maximum rated power	$P_{max}$	10 kW
Line frequency	$f_i$	60 Hz
Inductors	$L_R, L_S \& L_T$	300 $\mu$ H ~ 2 mH
Output filter capacitor	$C_o$	5 $\mu$ F
Power switch	IGBT G40N60A4	$V_{CE(on)}$ typ. = 1.7 V, $V_{CES}$ = 600V, and $I_{CTC=25^\circ C}$ = 75 A
Power diode (silicon carbide)	CREE C3D20060D	$V_{R(TJ=25^\circ C)}$ typ. = 1.5 V Zero Recovery Time
Switching frequency	$f_s$	20 kHz
DC-bus capacitance	$C_{DC}$	12*470 $\mu$ F

### A. Test with One Line-Cycle Regulation Approach

For the proposed voltage regulation test, a PV system combing 10 kW PV arrays, three maximum power point trackers (MPPT), and dc load (resistive load) with the proposed three-phase inverter prototype was implemented. In rectification mode, the measured inductor current and dc-bus voltage waveforms for dc load variation from no load to 800 W and from 800 W to 2 kW are shown in Fig. 12, in which the inverter only uses OLCRA to balance power flow. In grid-connection mode, even though OSLCRA can regulate abrupt voltage change, the MPPTs need a soft-start to avoid large inrush current, especially under high power level, which can insure system reliability. Fig. 13 shows waveforms of the three-phase inductor currents and dc-bus voltage under maximum power tracking to 7 kW ( $P_{max}$ ), and their expanded transient waveforms. It can be observed that the MPPTs can track the maximum power gradually due to soft start and the inverter tunes current command  $I_A(n)$  to regulate the dc-bus voltage with OLCRA. With the proposed OLCRA, the inverter can regulate the dc-bus voltage corresponding to the load line.

### B. Test with One-Sixth Line-Cycle Regulation Approach

The OSLCRA is used for regulating the dc-bus voltage under abrupt power imbalance. Thus, it is necessary to select a proper operating condition when adopting OSLCRA. According to the design of dc-bus capacitance, the maximum voltage variation within one-sixth line cycle is 13 V. For practical consideration, a 20 % voltage change within one-sixth line cycle is large enough to be an upper-bound condition. That is, when the voltage variation is higher than 2.6 V ( $\sim 13V*20\%$ ) over one-sixth line cycle, the control will enact OSLCRA to regulate the dc-bus voltage.

Fig. 14 shows a fast dc load variation from no load to 3 kW and from 3 kW to 1.5 kW with OSLCRA in rectification mode. It can be seen that the inverter controller just updates current command once at one-sixth line cycle and dc-bus voltage  $v_{DC}$  is regulated to its corresponding set-point voltage. However, under high power level, the error between the ideal current command for balancing power and the real one will become larger due to unpredictable time from power imbalance. Fig. 15 shows measured waveforms of the three-

phase inductor currents and dc-bus voltage during PV system regulation process, and their expanded waveforms when the MPPTs shutdown at 7 kW. It can be seen that the inverter controller updates current command immediately after the MPPTs shutdown but at wrong current level by the OLCRA. The unpredictable time from the MPPT shutdown will result in wrong current command at  $T/6$  and cause dc-bus voltage deviating from the load line. However, the inverter will tune the current command again to regulate the dc-bus voltage, as shown in Fig. 15(b), and the dc-bus voltage will come back to the load line.

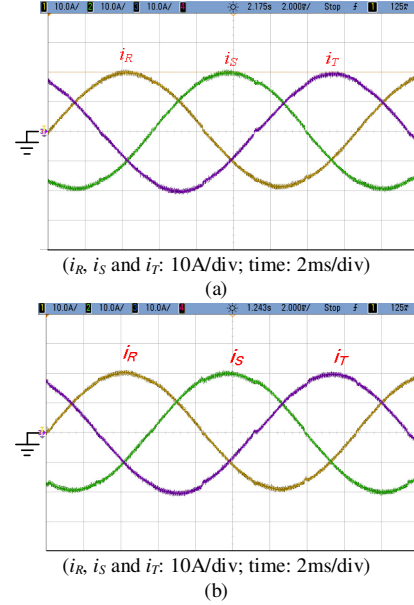


Figure 10. Measured waveforms of the three-phase inductor currents (a) with and (b) without considering wide inductance variation in grid-connection mode at 5 kW.

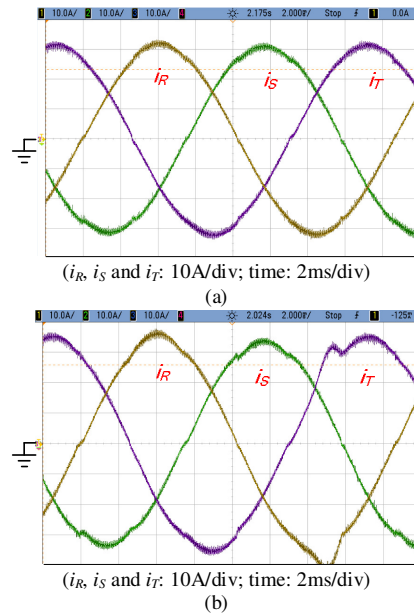


Figure 11. Measured waveforms of the three-phase inductor currents (a) with and (b) without considering wide inductance variation in grid-connection mode at 10 kW.

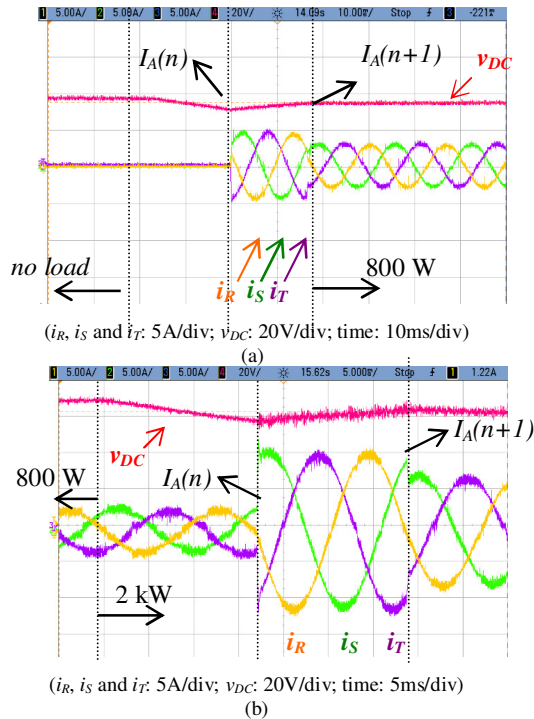


Figure 12. Measured waveforms of the three-phase inductor currents and dc-bus voltage  $v_{DC}$  for dc load variation (a) from no load to 800 W, and (b) from 800 W to 2 kW in rectification mode.

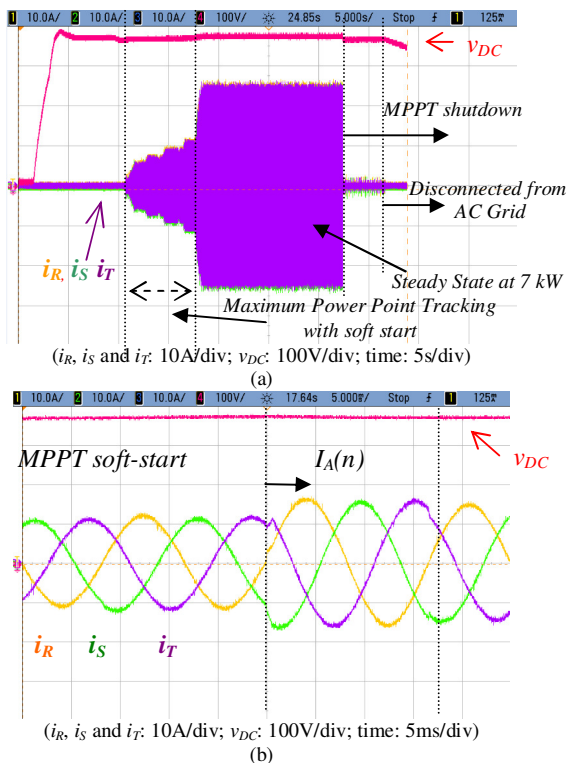


Figure 13. Measured waveforms of the three-phase inductor currents and dc-bus voltage (a) during PV system regulation process, and (b) their expanded waveforms during MPPT.

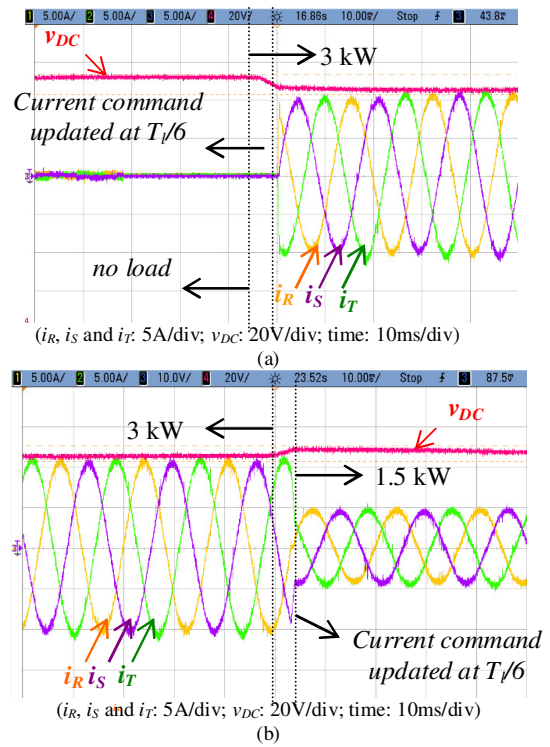


Figure 14. Measured waveforms of the three-phase inductor currents and dc-bus voltage  $v_{DC}$  for dc load variation (a) from no load to 3 kW, and (b) from 3 kW to 1.5 kW in rectification mode.

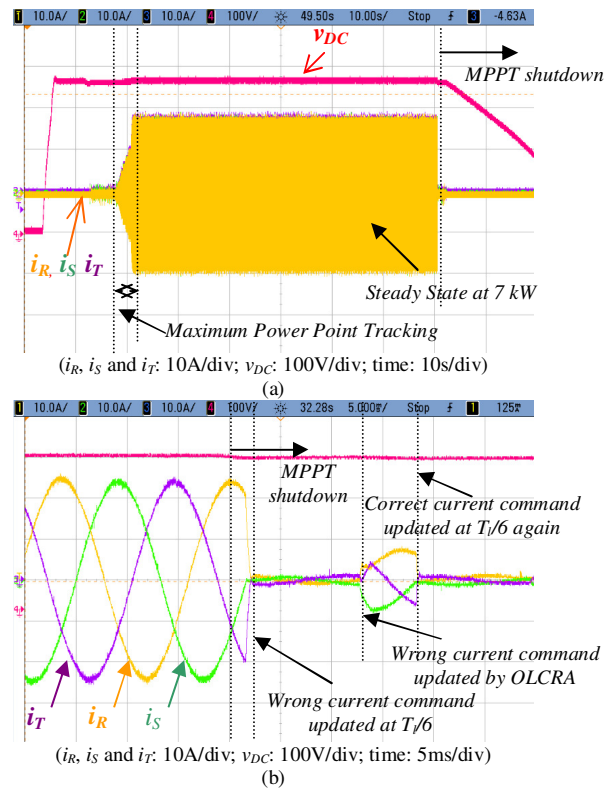


Figure 15. Measured waveforms of the three-phase inductor currents and dc-bus voltage (a) during PV system regulation process, and (b) their expanded waveforms at MPPT shutdown.

## V. CONCLUSIONS

A dc-bus voltage control for three-phase bi-directional inverters in dc-microgrid applications has been presented in the paper. The linear power management scheme including both grid-connection and rectification modes has been described in detail. In the paper, the one line-cycle regulation approach based on the linear power management scheme has been proposed for tuning current command cycle by cycle to regulate the dc-bus voltage according to the load line. For an abrupt voltage change, the one-sixth line-cycle regulation approach has been also proposed to prevent over/under dc-bus voltage fault, insuring system availability. Experimental results have verified the feasibility of the proposed dc-bus voltage control approaches.

## REFERENCES

- [1] T.-F. Wu, C.-H. Chang, L.-C. Lin, and C.-L. Kuo, "Power Loss Comparison of Single- and Two-Stage Grid-Connected Photovoltaic Systems," *IEEE Transactions on Energy Conversion*, 2011, vol. 26, no. 2, pp.707–715.
- [2] Z.-H. Ye, D. Boroyevich, K. Xing, and F.-C. Lee, "Design of parallel sources in Distributed Power Systems by Using Gain-Scheduling Technique," in *Proc. IEEE PESC*, 1999, pp. 161-165.
- [3] Y. Ito, Y. Zhongqing, and H. Akagi, "DC Microgrid Based Distribution Power Generation System," in *Proc. IEEE IPEDC'04*, 2004, pp.1740-1745.
- [4] A. Luo, C. Tang, Z. Shuai, X.-Y. Xu, and D. Chen, "Hierarchical Control of Droop-Controlled AC and DC Microgrid – A General Approach Toward Standardization," *IEEE Transactions on Industrial Electronics*, vol. 58, no. 1, pp. 158-172, 2011.
- [5] H. Kakigano, A. Nishino, and T. Ise, "Distributed Voltage Control for DC Microgrid with Fuzzy Control and Gain-Scheduling Control," in *Proc. IEEE ICPE*, pp. 256-263, 2011.
- [6] H. Kakigano, Y. Miura, and T. Ise, "Low-Voltage Bipolar-Type DC Microgrid for super High Quality Distribution," *IEEE Transactions on Power Electronics*, vol. 25, no. 12, pp. 3066-3075, 2010.
- [7] J.-S. Park, J.-K. Choi, B.-G. Gu, I.-S. Jung, E.-C. Lee, and K.-S. Ahn, "Robust DC-Link Voltage Control Scheme for Photovoltaic Power Generation System PCS," in *Proc. IEEE INTELEC*, pp. 1-4, 2009.
- [8] D. Salomonsson, L. Soder, and A. Sannino, "An Adaptive Control System for A DC Microgrid for Data Centers," *IEEE Transactions on Industrial Applications*, vol. 44, no. 6, pp. 1910-1917, 2008.
- [9] J.-S. Park, J.-K. Choi, B.-G. Gu, I.-S. Jung, E.-C. Lee, and K.-S. Ahn, "A Hybrid Renewable DC Microgrid Voltage Control," in *Proc. IEEE IPEDC*, pp. 725-729, 2009.
- [10] Z. Li, T. Wu, X. Yan, K. Sun, and J.M. Guerrero, "Power Control of DC Microgrid Using DC Bus Signaling," in *Proc. IEEE APEC* pp. 1926-1932, 2011.
- [11] N. Hur, J. Jung, and K. Nam, "A Fast Dynamic DC-Link Power-Balance Scheme for A PWM Converter-Inverter System," *IEEE Transactions on Industrial Electronics*, vol. 48, no. 4, pp. 794-1803, 2001.
- [12] J. Yao, H. Li, Y. Liao, and Z. Chen, "An Improved Control Strategy of Limiting the DC-Link Voltage Fluctuation for a Doubly Fed Induction Wind Generator," *IEEE Transactions on Power Electronics*, vol. 23, no. 3, pp. 1205-1213, 2008.
- [13] T.-F. Wu, L.-C. Lin, C.-H. Chang, Y.-L. Lin, and Y.-C. Chang, "Current Improvement for A 3  $\phi$  Bi-Directional Inverter with Wide Inductance Variation," in *Proc. IEEE ECCE Asia*, 2011, pp.1777–1784.